



Evolution characteristics of the rainstorm disaster chains in the Guangdong–Hong Kong–Macao Greater Bay Area, China

Yujie Wang^{1,2} · Ge Gao^{1,3} · Jianqing Zhai³ · Qiufeng Liu³ · Lianchun Song³

Received: 6 July 2022 / Accepted: 17 July 2023 / Published online: 22 September 2023
© The Author(s), under exclusive licence to Springer Nature B.V. 2023

Abstract

Enhancing the resistance of urban agglomeration against rainstorm-induced disasters has become a more urgent mission for the construction of the Guangdong–Hong Kong–Macao Greater Bay Area (GBA). But, few studies have focused on the rainstorm disaster chains at the scale of urban agglomeration. In view of this, in this study, we investigate the classification, mechanism, probability, variation and risk of rainstorm disaster chains in the GBA by using the meteorological observation, physical geography, land-use, socio-economic and disaster loss data during 1990–2018. The results show that the rainstorms can lead to many disaster chains in the GBA, such as flash flood, riverine flood, debris flow/landslide, urban waterlogging and agricultural waterlogging. Among them, the urban waterlogging disaster chain has the highest probability to occur. Furthermore, these disaster chains are influenced and exacerbated by each other, leading to cascading effects. Since the twenty-first century, the frequency of urban waterlogging has increased and becomes the most prominent rainstorm-induced disaster, while flash flood, riverine flood and debris flow/landslide decreased. The rainstorm disaster loss index in the GBA shows a significant increasing trend ($p < 0.05$) during 1990–2018. By jointly considering the rainstorm hazard, the exposure of disaster-bearing bodies and the sensitivity of disaster-pregnant environment, Shenzhen, Zhaoqing and Huizhou rank the top three in the frequency of rainstorm disaster chains, and Zhaoqing ranks the first in disaster loss index. In addition, the areas with high rainstorm disaster risk level increase with the augmentation of return period. Guangzhou, Zhaoqing and Shenzhen are at high-risk level for the rainstorm disasters with 10-year and 20-year return periods. We hope that this study can provide a scientific reference for the rainstorm disaster risk management in the GBA.

Keywords Rainstorm disaster chains · Risk · Evolution characteristics · Guangdong-Hong Kong-Macao Greater Bay Area

1 Introduction

Climate change has led to frequent extreme rainstorms and has brought great impacts on social–economic development in coastal cities in recent years (CanTERS et al. 2014; Silva et al. 2017; Zhou et al. 2017; Kang et al. 2018; Lyu et al. 2018; Islam and Raja 2021; Liu et al. 2022a). According to the atlas of mortality and economic losses from weather, climate and water extremes from 1970 to 2012 provided by the World Meteorological Organization, the frequency of rainstorm disasters accounted for 79% of all natural disasters, and the casualties and direct economic losses caused by rainstorm disasters accounted for 55% and 86% of the total, respectively (Golnaraghi et al. 2014). With global warming and economic development, the total global economic losses caused by rainstorm disasters will increase by 17% in the next 20 years in the absence of large-scale production structure adaptation (Willner et al. 2018). Rainstorm disasters are one of the most frequent natural disasters, often leading to chain reactions of multi-disasters (Kappes et al. 2012; Helbing 2013), and can bring substantial regional or global impacts (Hallegatte 2014; Levermann 2014; Samphantharak 2014). The rainstorm disaster chain is a process in which rainstorm causes losses and influences the disaster-bearing bodies (refer to the subjects of human society directly affected and damaged by disasters, such as life, property and infrastructure) under certain disaster-pregnant environment (refers to the comprehensive earth surface environment, including topographic conditions, river systems and underlying surface attributes). The rainstorm disaster chain usually triggers other derivative disasters and causes more complex influence on disaster-bearing bodies (Liu et al. 2021b). It has complex formation mechanisms and is featured by time continuity and spatial expansibility. The rainstorm disaster chain is triggered by multi-disasters that occur simultaneously or sequentially, so it is difficult to be forecasted. Therefore, it has attracted much attention from scholars.

However, the studies on the rainstorm disaster chain are few at present. Most of the related studies focused on the rainstorm variation characteristics, the formation mechanisms of rainstorm risk, the risk assessment methods and risk zoning (Qin et al. 2015; Metin et al. 2018; Sun et al. 2020). The studies on the rainstorm disaster chain mainly focused on individual cases (Wang et al. 2011; Ye et al. 2018; Wan et al. 2018) or a single disaster. For example, Du and Gu (2016) used a Bayesian network to build a flood disaster chain model and analyzed the chain effect of flood disaster. Wang et al. (2014) established a comprehensive evaluation model of urban flood risk based on a normal cloud model. Shi et al. (2017) evaluated the flood risk in typical years in Ankang City using a cloud model-based method. Wen et al. (2018) constructed a vulnerability curve model for the rainstorm and flood disasters in Hubei Province.

The Guangdong–Hong Kong–Macao Greater Bay Area (GBA) is one of the most economically developed and densely populated regions in China. Affected by the low-latitude sea–land interaction and the South China Sea monsoon, there are many types of frequent co-occurring meteorological disasters. Under the background of global climate change, rapid urbanization and economic development, the precipitation intensity (Zhang et al. 2012; Zhao et al. 2014; Liu et al. 2016), the exposure to rainstorm disasters (Chen et al. 2019; Wang et al. 2022), the impervious urban area (Yang et al. 2017; Feng and Fan 2018) and the influence of rainstorm and flood disasters (Chen et al. 2017; Zhou et al. 2019; Qin et al. 2021) have all increased in the Pearl River Basin, where the GBA is located. Wang et al. (2021) showed that the frequency of rainstorm disasters in the GBA in 2005–2018 increased by two times than that in 1990–2004. Furthermore, the extreme precipitation

indexes will increase, and the area proportion of the two highest flood risk levels will be as high as 60% in the mid-21st (Wang et al. 2021). The construction of GBA is a major national strategy, so it is of great significance to investigate the evolution characteristics of rainstorm disaster chains in the GBA.

Therefore, based on the comprehensive evaluation of the 990 cases of rainstorm-induced disasters from 1990 to 2018 in the GBA, this study investigates the classification and mechanism of rainstorm disaster chains, analyzes the spatiotemporal distribution and variation characteristics, establishes a quantitative function between disaster losses and three variables (hazard severity, geographical environment and exposure) by on the statistics correlation analysis and conducts rainstorm disaster risk assessment. We hope that this study can deepen the understanding of rainstorm disaster chains in the GBA and provide a scientific reference for the risk management of rainstorm disasters in the GBA.

2 Data and methods

2.1 Study area

Located in the southern coast of China, the GBA is composed of Hong Kong, Macau and nine cities of Guangdong Province, namely, Guangzhou, Foshan, Zhaoqing, Shenzhen, Dongguan, Huizhou, Zhuhai, Zhongshan and Jiangmen (Fig. 1). The total area of GBA is 56,000 square kilometers, which covers the lower reaches of the Pearl River Basin and part of the coastal regions of Guangdong Province. The water system in the

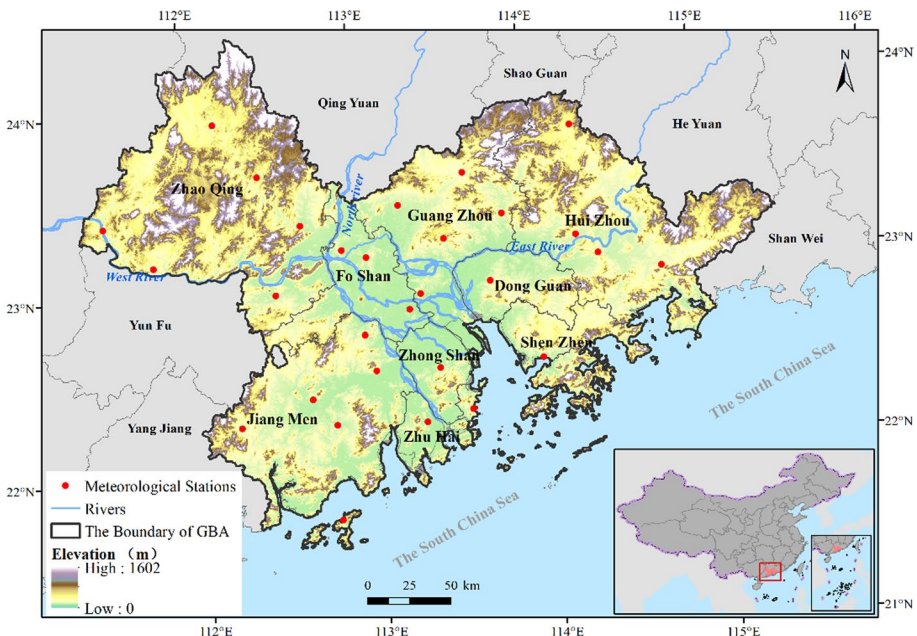


Fig. 1 Terrain and meteorological stations (red dots) in the GBA

GBA is complex, with dense and intertwined river networks. The soil is mainly granite-weathered red soil, and the underground is primarily a shallow covered karst area.

The GBA is located in the subtropical monsoon climate zone, with an average annual precipitation of 1886 mm, but the precipitation is unevenly distributed among different seasons, with less precipitation in winter and more precipitation in summer. The precipitation is the most in June (363 mm) and the least in December (38 mm), with a difference of nearly 10 times between them. The number of rainstorm day is also the highest in June (1.8 days) and the lowest in February, with less 0.1 days (Fig. 2). The rainy season in this region is long, and heavy rainstorm occurs frequently, causing serious disasters that affect widespread areas (Zhou et al. 2019).

2.2 Data

The daily observation data from 29 meteorological stations in the GBA from 1990 to 2018 (Fig. 1) are used in this study, which is from the Dataset of Daily Climate Data from Chinese Surface Stations for Global Exchange (V3.0) and has undergone strict quality control (Ren et al. 2012).

The river data and the elevation model of disaster-pregnant environment used in this study come from the 1:250,000 scale topographic database of National Basic Geographic Information Center (Wang et al. 2001). The 1-km resolution land-use data are from the Institute of Geography Sciences and Natural Resources, Chinese Academy of Sciences (Xu et al. 2018). The vegetation coverage data are calculated based on the 1-km normalized difference vegetation index products of the moderate resolution imaging spectroradiometer. Population and gross domestic product (GDP) data are from the Guangdong Statistical Yearbook.

According to the classification of meteorological disasters by the China Meteorological Administration (CMA 2020), the disasters caused by typhoon-induced rainstorms are categorized as typhoon disasters. Therefore, the rainstorm disaster chains investigated in this study are those caused by non-typhoon-related rainstorms. The disaster loss data caused by rainstorms are from the meteorological disaster database of the National Climate Center of China Meteorological Administration, including direct economic loss, disaster-affected population and casualties (Li and Zhao 2022).

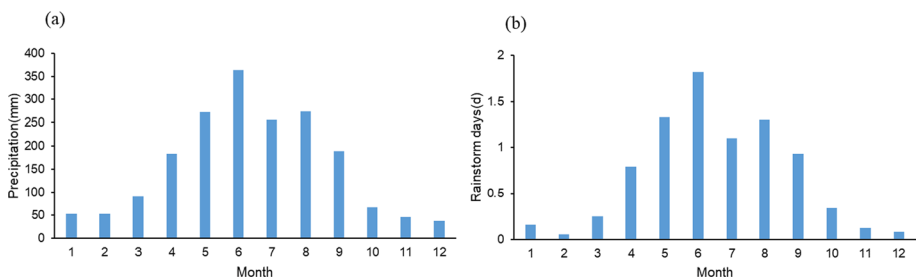


Fig. 2 Monthly precipitation and rainstorm days averaged from 1990 to 2018 in the GBA

2.3 Methods

2.3.1 Normalization

In order to make the scales of different indicators comparable, the normalization is conducted for all the elements in this study. The equation is as follows (Eq. (1)) (Wang et al. 2022):

$$XD_i = 0.5 + 0.5 \times \frac{X_i - X_{\min}}{X_{\max} - X_{\min}} \quad (1)$$

where XD_i denotes the normalized value of the i th element, X_i is the i th element value, X_{\min} is the minimum of the element and X_{\max} is the maximum of the element.

2.3.2 Hazard index

The rainstorm-induced disasters investigated in this study are those caused by non-typhoon-related rainstorms. According to the grade of precipitation (GB/T 28592–2012), a day with daily precipitation greater than or equal to 50 mm is defined as a rainstorm day. If one at least meteorological station in the monitoring area has a rainstorm, the 1st day of the rainstorm process will be judged as the beginning date. After the rainstorm process starts, if there is no rainstorm in the monitoring area on a single day, and the day before it is the rainstorm process end date. Referring to the previous quantitative evaluation methods for the comprehensive intensity of rainstorm process (Ye et al. 2019; Wu et al. 2019), three factors of rainstorm such as intensity, duration and coverage range are selected to evaluate the rainstorm dangerousness in this study.

The rainstorm hazard index (H) reflects the degree of rainstorm hazard. It is calculated by the average rainfall intensity (I , unit: mm), average coverage range (C , unit: station) and duration (D , unit: day) of a rainstorm process as follows:

$$H = I\sqrt{C}\sqrt{D} \quad (2)$$

where I denotes the average precipitation of all the rainstorm stations during the rainstorm process; C is the daily average number of stations with rainstorm during the rainstorm process and D is the number of days from the start date to the end date of the rainstorm process. H is normalized to get the standardized value of rainstorm hazard index, and the annual rainstorm hazard index is the accumulation of all the standardized values of the rainstorm hazard index in that year.

2.3.3 Exposure index

The previous research suggested to use the population density or per unit of GDP as the exposure indicator (Li et al. 2021). In this study, both indicators of per unit of population and GDP at 1-km grid spacing in the GBA are used to establish the exposure index (EX). According to Wang et al. (2021), EX is calculated as follows:

$$EX = 0.5 \times \text{POP}_N + 0.5 \times \text{GDP}_N \quad (3)$$

where POP_N denotes the normalized data of the population per square kilometer, and GDP_N is the normalized data of the GDP per square kilometer. The entire region and each city of the GBA are calculated according to their own POP_N and GDP_N .

2.3.4 Disaster-pregnant environment index

The previous research suggested that terrain, land cover/land use, river network density, infrastructure and drainage pipeline density are the environment factors that relate to rainstorm disasters (Sun et al. 2020; Islam and Raja 2021; Li et al. 2021). Here, we adopt the method of Wang et al. (2021) to calculate disaster-pregnant environment index (EN).

$$EN = 0.4 \times T + 0.3 \times RI - 0.3 \times VC \quad (4)$$

where T , RI and VC are normalized terrain index, river network density index and vegetation coverage, respectively. The values of the entire region and each city of the GBA are obtained by calculating the average over the grid points within their respective administrative areas.

2.3.5 Disaster loss index

In order to evaluate the comprehensive disaster losses of rainstorm disasters, the concept of disaster loss index is introduced in this study. Based on the disaster loss data such as disaster-affected population, casualties and direct economic loss, the disaster loss index of each disaster-causing rainstorm is calculated by the method of Zhou et al. (2017), as shown in Eq. (5).

$$DL = \log_{10}(P + 1) + 10 \frac{L}{GDP} + 10 \frac{AP}{POP} \quad (5)$$

where DL represents the disaster loss index, P is the number of casualties, L is the direct economic loss, GDP is the gross domestic product, AP is the disaster-affected population and POP is the total population. The annual disaster loss index of rainstorm is the accumulation of all disaster loss indexes of rainstorm within the year.

2.3.6 Risk assessment

The disaster risk factors mainly include hazard intensity, exposure of disaster-bearing body and sensitivity of disaster-pregnant environment (Cardona et al. 2012). The risk assessment of rainstorm disaster loss is constructed based on hazard index, exposure index and disaster-pregnant environment index (Shi 2005), as shown in Eq. (6):

$$DL = f(H, EX, EN) \quad (6)$$

We use the regression method to establish a loss function of the relationship between disaster loss index and hazard index. Based on the normal distribution function of hazard index, the thresholds for the return periods of 5, 10 and 20 years are calculated in the study. Combined with multi-year averaged exposure index and disaster-pregnant environment index, the DL for different return periods is estimated according to the loss function.

3 Results

3.1 Rainstorm disaster chains

3.1.1 The structure of rainstorm disaster chains

The disaster chain is a complex system, which consists of disaster-inducing factor, disaster-pregnant environment and disaster-bearing body. The disaster losses are affected by the joint effect of the hazard severity of disaster-inducing factor, the sensitivity of disaster-pregnant environment and the exposure of disaster-bearing body (Shi 2005). Due to the complex geographical environment, the rainstorm disasters in the GBA are very complex, often presenting a chain effect. When the rainstorm intensity reaches the disaster threshold, different rainstorm disaster chains are triggered in different disaster-pregnant environment. According to the historical records of rainstorm-induced disasters in the GBA, the rainstorm disaster chains mainly include flash flood, riverine flood, debris flow or landslide, urban waterlogging and agricultural waterlogging (Fig. 3). Moreover, they are influenced and exacerbated by each other, leading to cascading effects in different disaster-bearing bodies. For example, flash flood could trigger debris flow/landslide, riverine flood, urban waterlogging and farmland waterlogging. Riverine flood can aggravate urban and farmland waterlogging. The rainstorm disaster chains can lead to the breaking of embankments, the destroy of bridges and culverts, the collapse of houses, flooding of farmland, damage to infrastructures (such as power, communication, water conservancy and roads) and waterlogging in urban streets and farmland. Ultimately, they cause casualties, agricultural reduction, industrial shutdown, interruptions in transportation, power and communications and economic and property losses.

Taking the heavy rainstorm on May 5–7, 2010, in the GBA as an example, it triggered all rainstorm disaster chains which were exacerbated by each other. The 3-h and 6-h rainfall intensities exceeded 50-year return period in some meteorological stations of Guangzhou, Huizhou and Dongguan. The rainstorm resulted in the outbreak of mountain flash flood in Huizhou, triggered debris flows/landslides and aggravated serious riverine flood in the North River tributary. The heavy rainstorm and the riverine flood led to severe urban

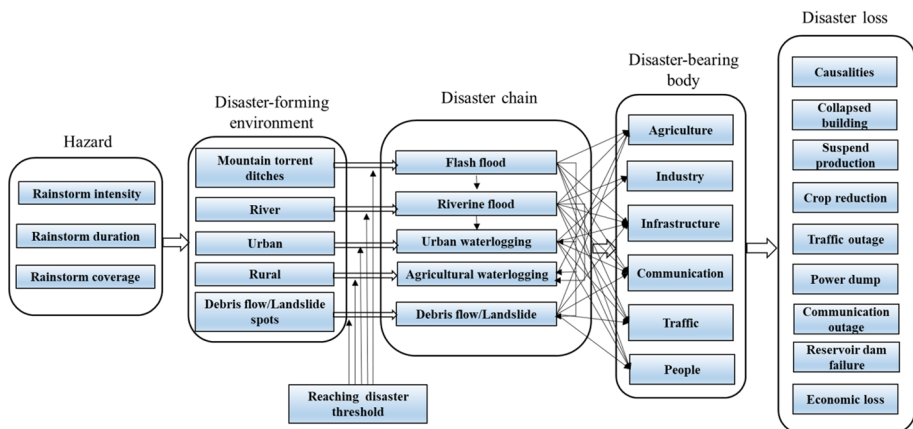


Fig. 3 Structures of the rainstorm disaster chains in the GBA

waterlogging in Guangzhou, Shenzhen and Dongguan. In Guangzhou, the rainstorm disaster chains resulted in six deaths, 13,000 vehicles soaked, 17,120 ha farmland flooded and 544 million yuan of direct economic losses.

3.1.2 Rainstorm disaster loss

The meteorological disaster database provided by the National Climate Center of China Meteorological Administration has been statistically analyzed in this study. The results show that in the GBA from 1990 to 2018, the rainstorm disaster chains caused an average of 326,000 people affected, 14 people died and a direct economic loss of 1.35 billion yuan (calculated at 2018 constant prices) each year (Fig. 4). The direct economic loss was the largest in 1994, reaching 7.82 billion yuan, followed by 7.29 billion yuan in 2008. The affected population was the largest in 2008 (2.57 million people), followed by 1994 (1.12 million people). In terms of the death toll from rainstorm disasters, the number was the largest in 1998 (88), followed by 1997 (80). From 1990 to 2018, the rainstorm disaster loss index in the GBA shows a significant increasing trend ($p < 0.05$), and the inter-annual fluctuation is large. In 2005, 2006, 2014 and 2008, the rainstorm disaster index is relatively large, exceeding 40. However, in 1991, 1990, 1995 and 1999, it is relatively small, less than 10 (Fig. 4d).

From the multi-year average comprehensive disaster loss index of each city during 1990–2018 (Table 1), it can be seen that Zhaoqing has the largest index (5.22), followed by Foshan (3.99) and Huizhou (3.49), while the index in Zhuhai, Zhongshan and Dongguan is relatively small (less than 2). This is because the multi-year average proportion of economic losses to GDP (0.37%) and the multi-year average proportion of affected population to total population (21.9%) caused by rainstorm disasters are the highest in Zhaoqing, while they are relatively low in Zhongshan (0.11% and 3.4%, respectively) and Dongguan

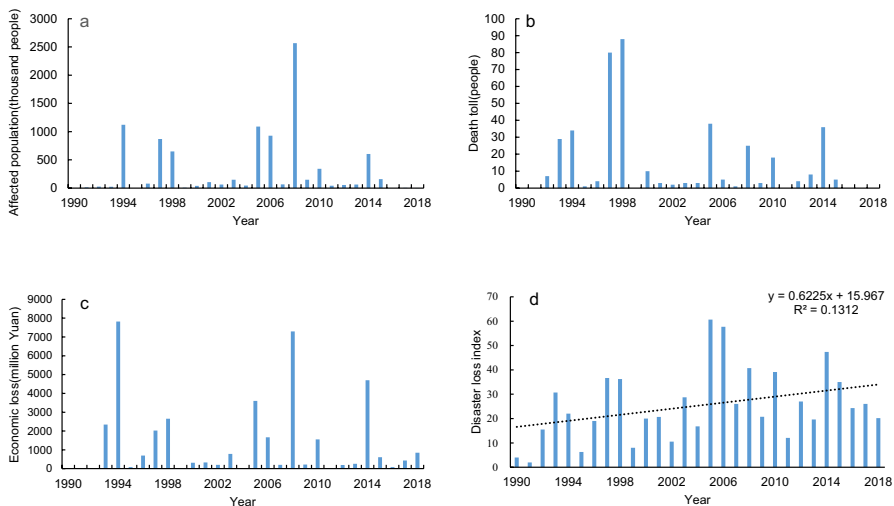


Fig. 4 The annual **a** disaster-affected population, **b** death toll, **c** direct economic loss and **d** comprehensive disaster loss index in the rainstorm processes in the GBA from 1990 to 2018

Table 1 Multi-year averages of the rainstorm hazard index (*H*), the exposure index of hazard-bearing bodies (*EX*), the disaster-pregnant environment index (*EN*) and the disaster loss index (*DL*) for each city of the GBA during 1990–2018

City	<i>H</i>	<i>EX</i>	<i>EN</i>	<i>DL</i>
Dongguan	3.41	0.61	0.45	1.73
Foshan	5.84	0.57	0.54	3.99
Guangzhou	8.69	0.55	0.34	3.22
Huizhou	6.70	0.51	0.22	3.49
Shenzhen	8.23	0.72	0.27	2.47
Jiangmen	2.95	0.51	0.30	2.62
Zhaoqing	7.71	0.50	0.13	5.22
Zhongshan	3.06	0.56	0.52	1.58
Zhuhai	5.39	0.54	0.37	0.98

(0.14% and 11.0%, respectively). Moreover, the rainstorm hazard is relatively high in Zhaoqing and low in Zhongshan and Dongguan. The reasons are discussed in detail in Sect. 3.2.

3.1.3 The probability of rainstorm disaster chains

From 1990 to 2018, there are 990 rainstorm disasters in the GBA. Among them, the occurrence frequency of flash flood, riverine flood, debris flow/landslide, urban waterlogging and agricultural waterlogging is 25, 145, 193, 629 and 463, respectively (Table 2). It can be seen that the probability of urban waterlogging disaster is the highest, accounting for 63.5% of the total rainstorm disasters, which is related to the rapid expansion of urban impervious surface in the GBA (Feng and Fan 2018). The second is the agricultural waterlogging disaster (46.8%). The occurrence probability of debris flow/landslide ranks the third (19.5%), which is due to the fact that there are more than 70 hidden danger points of geological disasters in the GBA, accounting for about 80% of all hidden danger points in Guangdong (Department of Natural Resources of Guangdong Province 2018). The occurrence probability of riverine flood disasters accounts for 14.6%, while that of flash flood disaster is relatively small (only 2.5%), mainly concentrated in the Zhaoqing mountainous area.

Table 2 Frequency of rainstorm disaster chains in the GBA during 1990–2018

City	Disaster frequency	Flash flood	Riverine flood	Urban waterlogging	Agricultural waterlogging	Debris flow/landslide
Dongguan	25	0	2	16	18	1
Foshan	134	1	30	48	62	48
Guangzhou	113	4	15	87	54	14
Huizhou	142	1	18	117	69	9
Shenzhen	264	5	10	233	9	70
Jiangmen	89	2	12	32	79	8
Zhaoqing	185	10	53	69	141	39
Zhongshan	24	2	5	18	20	4
Zhuhai	14	0	0	9	11	0
GBA	990	25	145	629	463	193

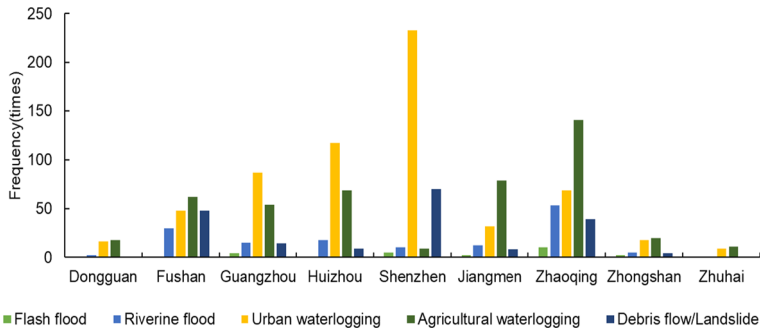


Fig. 5 The frequency of rainstorm disaster chains in the GBA cities from 1990 to 2018

As shown from Fig. 5, the frequency of rainstorm disasters in Shenzhen is the highest, reaching 264 and accounting for 26.7% of the total rainstorm disasters in the GBA. Among them, the frequency of urban waterlogging is the highest, accounting for 88%. This is consistent with the conclusion of Zhou et al. (2017), mainly due to the increase in rainstorm hazard. Debris flow/landslide ranks the second in Shenzhen (26.5%). Shenzhen is located in the coastal low-mountain and hilly area, with large undulating terrain and complex geological structure. Its eastern area is distributed with soluble rock, while the western area (Bao'an District and Nanshan District) is covered by soft soil. Therefore, heavy rainfall is prone to cause landslide disasters in Shenzhen (Tang 2016).

There are 185 rainstorm disasters in Zhaoqing from 1990 to 2018, accounting for 18.9% of the total frequency in the GBA and ranking the second. Among them, the frequency of agricultural waterlogging disaster is the highest (76.2%), followed by urban waterlogging (37.3%) and riverine flood (28.6%) and. The frequency of rainstorm disasters in Huizhou ranks the third in the GBA, accounting for 14.3%. Among them, urban waterlogging and agricultural waterlogging disasters account for 82.4% and 48.6%, respectively. Foshan has experienced a total of 134 rainstorm disasters in the past 30 years, of which agricultural waterlogging disasters account for 46.3%, urban waterlogging and debris flow/landslide account for 35.8%, respectively. Since 1990, there have been 114 and 89 rainstorm disasters in Guangzhou and Jiangmen, respectively, mainly urban waterlogging and agricultural waterlogging disasters. The frequencies of rainstorm disasters in Dongguan, Zhongshan and Zhuhai are all less than 30, mainly agricultural waterlogging disasters and urban waterlogging disasters.

The frequency of urban waterlogging disasters in GBA cities is the highest in Shenzhen, accounting for 37.0% of the total frequency of urban waterlogging disasters in the GBA, followed by Huizhou (18.6%). The frequency of agricultural waterlogging disasters is highest in Zhaoqing, accounting for 30.5%, followed by Jiangmen (17.1%). The most frequent geological disasters, such as landslides and debris flows, are also in Shenzhen, accounting for 36.3%, followed by Foshan (24.9%). The frequency of riverine flood disasters is the highest in Zhaoqing, accounting for 36.6%, followed by Foshan (20.7%). Flash flood disasters occur most in Zhaoqing, accounting for 40.0%, followed by Shenzhen (20.0%).

Table 3 Frequency of compound rainstorm disaster chains in the GBA from 1990 to 2018

City	1 chain	2 chains	3 chains	4 chains	Total
Dongguan	14	10	1	0	25
Foshan	85	43	6	0	134
Guangzhou	63	41	7	2	113
Huizhou	86	40	16	0	142
Shenzhen	208	49	7	0	264
Jiangmen	57	22	8	2	89
Zhaoqing	85	73	27	0	185
Zhongshan	5	13	6	0	24
Zhuhai	8	6	0	0	14
GBA	611	297	78	4	990

3.1.4 Compound rainstorm disaster chain

As mentioned in Sect. 3.1.1, the different rainstorm disaster chains in the GBA can be triggered by each other. According to historical records, the rainstorm disasters often appear as compound rainstorm disaster chain. Table 3 shows that among the rainstorm-induced disasters during 1990–2018, the frequency of 2, 3 and 4 disaster chains in simultaneity is 297, 78 and 4, accounting for 30%, 7.9% and 0.4% of the total frequency in the GBA, respectively. The city with the most frequent occurrence of two or more disaster chains is Zhaoqing, accounting for 54.1% of its total rainstorm disasters. Although the total frequency is not high in Zhongshan, the proportion of compound disaster chains is the highest, reaching 79.2%. The concurrence of four disaster chains only appears in Guangzhou and Jiangmen.

3.1.5 The variations of rainstorm disaster chains

Figure 6 shows the interdecadal variations of the frequency of rainstorm disaster chains in the GBA. As can be seen, the frequency in the 1990s, 2000s and 2010s is 211, 343

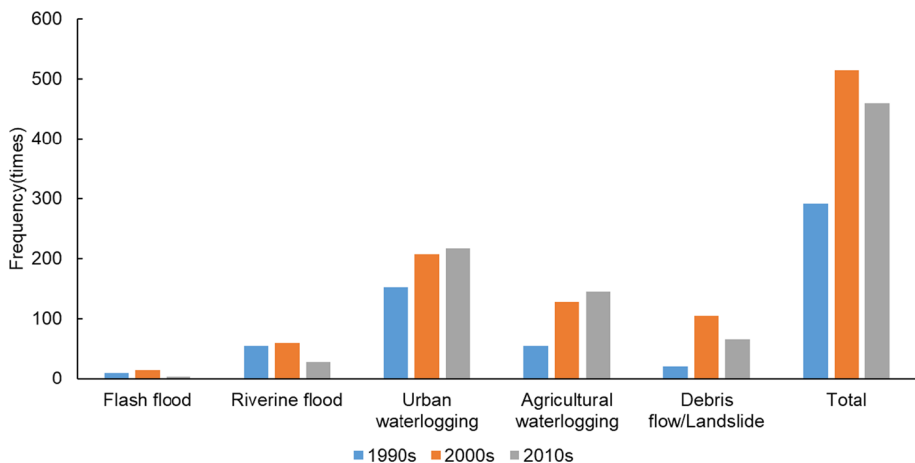


Fig. 6 The interdecadal variations of rainstorm disaster chains in the GBA

and 436 with an increasing trend. In the 1990s, 2000s and 2010s, the frequency of urban waterlogging disasters is 122, 178 and 329, respectively, and the frequency of agricultural waterlogging disasters is 106, 163 and 194, respectively. It can be seen that the frequency of urban waterlogging and agricultural waterlogging disasters shows an increasing trend, while the frequency of flash flood, riverine floods and debris flow/landslide is the highest in the 2000s and decreases in the 2010s. This may be related to the enhanced capacity of flood defense for small- and medium-sized rivers and of prevention to flash flood, debris flow/landslide in recent years (Yu and Li 2010; Zhao et al. 2022).

3.2 The variations of rainstorm hazard

Affected by the monsoon climate, the monthly variation of rainstorms in the GBA is obvious (Fig. 7). Seen from the multi-year average of 1990–2018, the frequency of rainstorm processes is the most in May (4.6 times), followed by June (4.3 times) (Fig. 7a). This is related to the frontal precipitation during the pre-flood season in South China and the onset of the South China Sea monsoon (Zhou et al. 2019). Besides, the largest number of monthly duration of rainstorm process days appears in June (12.1 days), followed by May (9.3 days) (Fig. 7b). The average intensity of rainstorm processes in May is the largest (76.3 mm), followed by June (75.6 mm) (Fig. 7c). The largest average impact range of

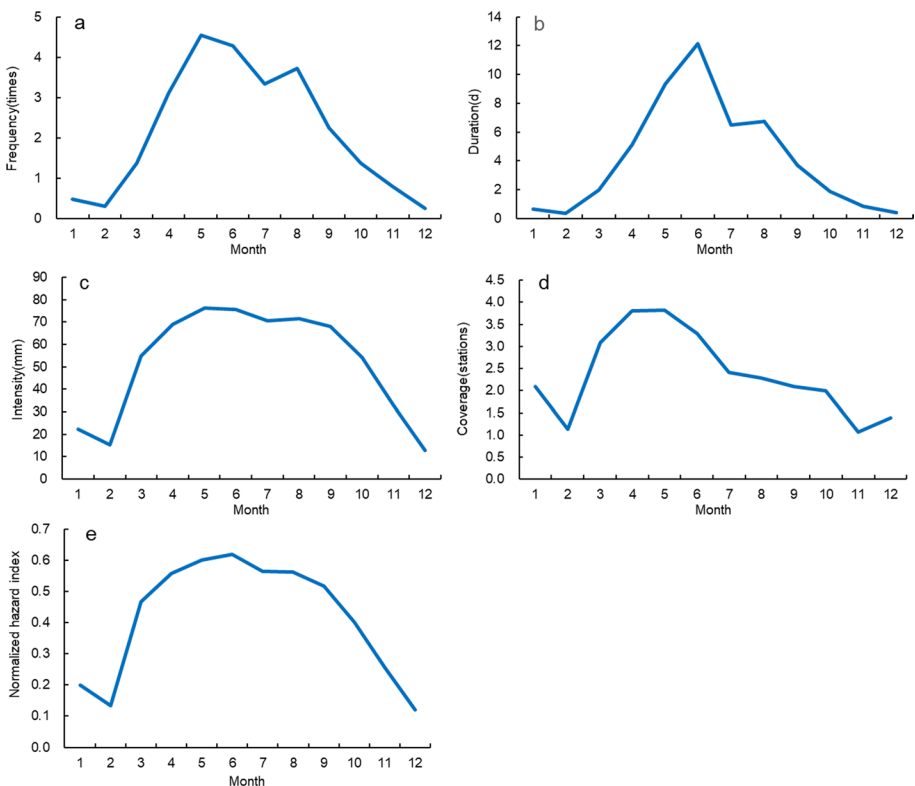


Fig. 7 Monthly **a** rainstorm frequency, **b** duration, **c** averaged intensity, **d** averaged coverage and **e** normalized and averaged hazard index of rainstorm processes in the GBA averaged in 1990–2018

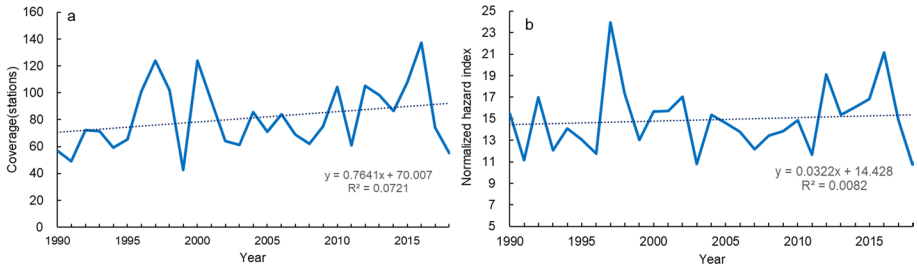


Fig. 8 Annual **a** coverage stations of rainstorm processes and **b** accumulated normalized hazard index in the GBA during 1990–2018

rainstorm processes is in April and May, both about 3.8 stations (Fig. 7d). According to Eq. (2), the hazard index of all rainstorm processes in the GBA from 1990 to 2018 is calculated, normalized and averaged by month, and then, the multi-year average hazard index of each month is calculated (Fig. 7e). The results show that the maximum value is in June, reaching 0.62, which is related to the intensity and long duration of the rainstorm processes in June. The second largest index appears in May (0.60), which is related to the frequent and wide-ranging rainstorms in May.

From 1990 to 2018, annual coverage stations of rainstorm processes tend to increase with a rate of $7.6 \text{ stations } 10\text{a}^{-1}$ (Fig. 8a), and the annual days of rainstorm processes in the GBA also show a slightly increasing trend with an increase rate of $1 \text{ day } 10\text{a}^{-1}$. The rainstorm hazard index in the GBA also shows a similar slightly increasing trend (Fig. 8b) and has close relationship with the above-mentioned indexes. The highest value appears in 1997 (24.0) and the lowest value in 2018 (10.7). The increased rainstorm hazard in the GBA is also related to the slight increase in precipitation intensity in the central and eastern Pearl River Basin since the 1990s (Zhang et al. 2012; Zhao et al. 2014).

From 1990 to 2018, the rainstorm hazard index in Dongguan, Foshan, Zhongshan, Guangzhou, Zhaoqing and Huizhou shows an increasing trend. The hazard index in Dongguan and Foshan increases significantly which has passed the significance test at 0.05 level, while the hazard index in Jiangmen, Shenzhen and Zhuhai shows a slight decreasing trend (Fig. 9). As shown from Table 1, the multi-year averaged annual rainstorm hazard index in 1990–2018 is the largest in Guangzhou, followed by Shenzhen and Zhaoqing, while that in Jiangmen and Zhongshan is relatively small.

3.3 The variations of exposure index

The population density in the GBA increased significantly from 1990 (425 persons km^{-2}) to 2018 (1057 persons km^{-2}) at a rate of 228 persons km^{-2} per 10 years (Fig. 10a), which has passed the significance test at 0.01 level. The city with the highest population density (4000 persons km^{-2} on average) and the fastest growing speed is Shenzhen (1925 persons km^{-2} per 10 years), followed by Dongguan City (1022 persons km^{-2} per 10 years) (Fig. 10b). In the past 30 years, the GDP per square kilometer in the GBA has also increased significantly with an increase rate of 51.38 million yuan per 10 years, which has passed the significance test at 0.01 level. The GDP has increased from 1.3 million Yuan km^{-2} in 1990 to 148.72 million Yuan km^{-2} in 2018, which means an increase of more than 100 times (Fig. 10c). Among them, Shenzhen has the fastest growth, with the increase

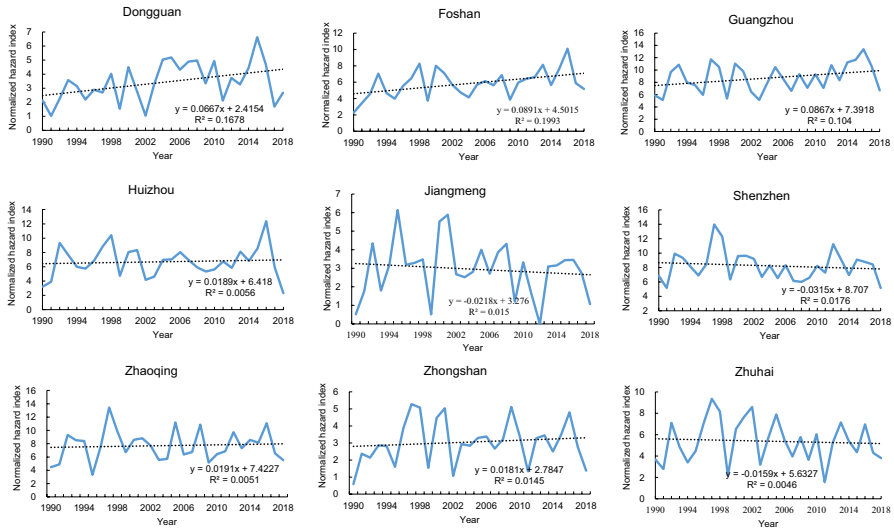


Fig. 9 The variation of rainstorm hazard index in the GBA cities from 1990 to 2018

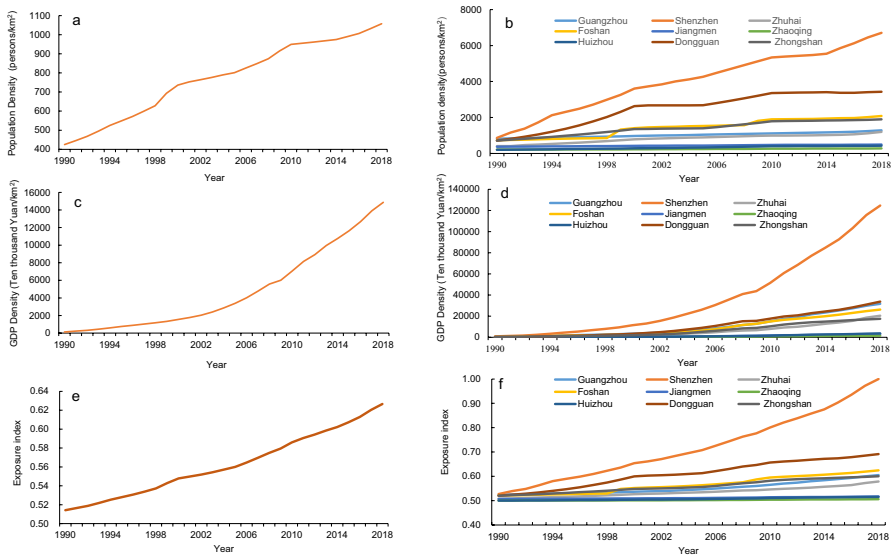


Fig. 10 The variations of **a** population density in the GBA, **b** population density of each city, **c** GDP density in the GBA, **d** GDP density in each city, **e** exposure index of the GBA and **f** exposure index of each city from 1990 to 2018

in average GDP per unit area being 400 million per 10 years. Zhaoqing, Jiangmen and Huizhou have relatively small GDP, which is 14.78 million, 30.97 million and 36.25 million Yuan km⁻² in 2018, respectively (Fig. 10d), and the growth rate is also small, all less than 10 million Yuan km⁻² per 10 years.

Equation (1) is used to normalize the GDP per unit area and population density in each city in the GBA, and then, the exposure index of the GBA and each city in 1990–2018 is calculated according to Eq. (3). It can be seen that the exposure index in the GBA has increased almost linearly from 1990 to 2018, with a tendency rate of 0.04 per 10 years (Fig. 10e). Among them, the tendency rate of exposure index in Shenzhen reaches 0.16 per 10 years, and the increase is the fastest among the nine cities. Meanwhile, the multi-year average of exposure index reaches 0.72 and is also the highest (Table 1), followed by Dongguan (0.61) and Foshan (0.57). Zhaoqing has the lowest average exposure index (0.50), with little change in the past 30 years (Fig. 10f).

3.4 The variations of disaster-pregnant environment

Since there are only vegetation coverage data in 1990, 1995, 2000, 2005, 2010, 2015 and 2018, when Eq. (5) is used to calculate the disaster-pregnant environment index in the GBA, and in each city, the calculation results represent the periods of 1990–1992, 1993–1997, 1998–2002, 2003–2007, 2008–2012, 2013–2016 and 2017–2018. Figure 11 shows that during these seven periods, the vegetation coverage area of the GBA shows a significant decreasing trend, and the decreasing rate is $7932 \text{ km}^2 \text{ 10a}^{-1}$ ($p < 0.01$). The vegetation coverage area of the GBA in 2018 ($43,313 \text{ km}^2$) is 9.4% less than that in 1990 ($48,031 \text{ km}^2$) (Fig. 11a). The vegetation coverage in GBA cities also shows a decreasing trend. Compared with 1990, the vegetation coverage area has decreased by 48.2% in Dongguan and by 37.7% in Shenzhen (Fig. 11b). For the average vegetation coverage area of the seven periods, Zhaoqing has the largest area, reaching $13,976 \text{ km}^2$, followed by Huizhou ($10,358 \text{ km}^2$), while Zhongshan, Zhuhai and Shenzhen have only about 1000 km^2 .

The multi-year average of the disaster-pregnant environment index in each city shows (Table 1) that Foshan has the highest index (0.54), followed by Zhongshan (0.52), while Zhaoqing has the lowest index (0.13). From the perspective of variations over the years,

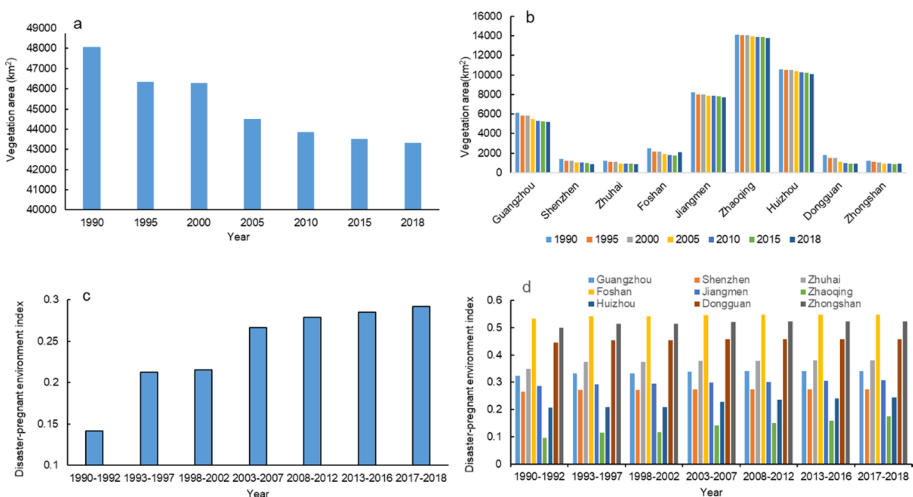


Fig. 11 The variations of **a** vegetation coverage area in the GBA, **b** vegetation coverage area in each city, **c** the disaster-pregnant environment index in the GBA and **d** the disaster-pregnant environment index in each city from 1990 to 2018

the index of the disaster-pregnant environment in both the GBA and the cities of GBA has shown an increasing trend, especially in Zhuhai and Zhongshan (Fig. 11c and d).

3.5 Risk assessment

According to Eq. (6), we construct the loss function. Through the statistical analysis of the linear correlations of the disaster loss index to the hazard index, the exposure index and the disaster-pregnant environment index, it is found that most of the correlation coefficients present positive correlation in nine cities of the GBA. The correlation coefficient between disaster loss index and hazard index is much higher than that of the other two factors. Therefore, the following two equations are adopted to construct the disaster loss assessment model based on all rainstorm-induced samples from 1990 to 2018 in nine cities of the GBA.

$$DL = a_0 + a_1H \quad (7)$$

$$DL = a_0 + a_1H + a_2H^2 \quad (8)$$

where a_0, a_1 and a_2 represent fitting parameters ($a_0 = 0.5971, a_1 = 0.4853$ in Eq. 7, $a_0 = 0, a_1 = 0.7847, a_2 = -0.0261$ in Eq. (8)). The fitting correlation coefficients are 0.531 and 0.548, which have passed the 95% significance test.

On this basis, we estimate the rainstorm disaster losses caused by the hazards in different return periods. First, we use the Kolmogorov–Smirnov method to check whether the time series of hazard index follows a normal distribution. The results suggest that they pass the significance test in all nine cities ($p < 0.05$). Second, we calculate the hazard thresholds of different return periods (5, 10 and 20 years). Then, we estimate the disaster loss index (DL) based on Eqs. (7) and (8). Last, the DL is divided into four levels in terms of the 50, 70 and 80 percentiles, namely, low risk ($DL \leq 2.5$), medium risk ($2.5 < DL \leq 4$), higher risk ($4 < DL \leq 5.5$) and high risk ($DL > 5.5$).

As can be seen from the DL risk levels in different return periods (Fig. 12), the areas of high risk in the GBA increase with the augmentation of return period. According to Eq. (7), Guangzhou is at high-risk level for all three return periods. For the 20-year return period, Huizhou, Shenzhen and Zhaoqing, except Guangzhou, are also at high-risk level. Dongguan, Zhongshan and Jiangmen are always at medium-risk level, while Foshan and Zhuhai are at higher risk level for different return periods. The assessment results based on Eq. (8) are remarkably different from those of Eq. (7). The risk levels of each city are medium or higher for 5-year return period. Only Guangdong is at high-risk level for 10-year return period. For 20-year return period, Guangdong, Shenzhen and Zhaoqing are at high-risk level. Since the risk assessment is based on the DL , it is basically in line with the actual loss situation.

4 Discussion

Many past studies evaluated the flood risk from the perspective of a single disaster such as urban waterlogging or river flooding (Zhou et al. 2017; Sun et al. 2020; Islam and Raja 2021; Li et al. 2021; Liu et al. 2021a). Different from the past studies, in this study, we assess the rainstorm-induced disasters on the basis of disaster chains. This study

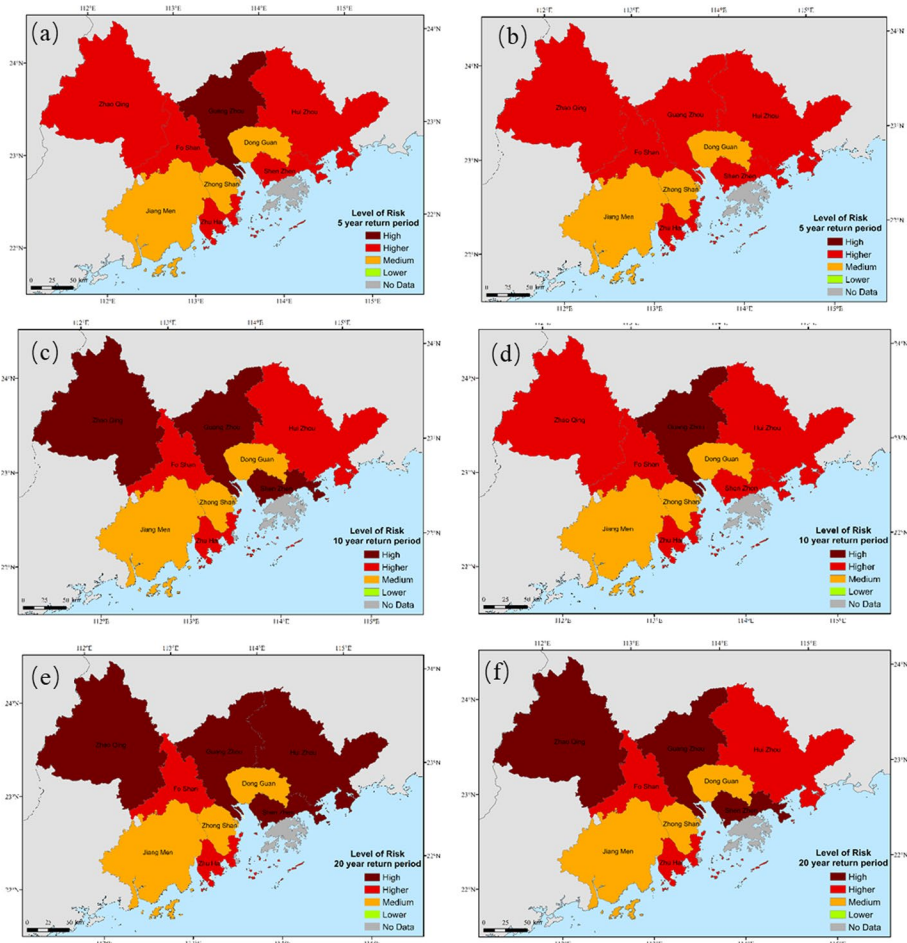


Fig. 12 Rainstorm disaster risk map in the GBA for different return periods. **a, c** and **e** are based on Eq. (7); **b, d** and **f** are based on Eq. (8)

innovatively investigates the classification, probability and mechanisms of rainstorm disaster chains, and assesses the variation and risk of rainstorm disaster chains at the scale of urban agglomeration. The results of this study can help local government to conduct macro decision-making on rainstorm disaster risk management.

The rainstorm-induced disaster is a complex issue and is affected by various factors (Quan 2014; Islam and Raja 2021; Liu et al. 2021b). In this study, several factors are selected from three aspects. However, these cannot fully reflect the influence factors of rainstorm disaster chains. As for rainstorm hazard, it is not only related to daily precipitation but also the precipitation intensity within a short period (Ye et al. 2018). As the meteorological observation data have limitations in spatial resolution, the hazard index should be calculated at the grid scale on the basis of more rain gauges. In the assessment of disaster-pregnant environment, the adopted factors such as terrain, river network and vegetation coverage all belong to natural conditions, while the differences in urban adaptability such as drainage condition are not considered (Islam and Raja 2021). In addition, this study

mainly considers the consequences of rainstorm disaster chain risk and ignores the coping capacities or resilience of social and economic dimensions.

The risk of rainstorm disaster is the result of the interactions among multiple influencing factors and compound rainstorm disaster chains, while some factors cannot be accurately described by mathematical models (Fang et al. 2015). It is quite difficult to delve into the specific interplay or interactions among these disaster chains. Furthermore, rainstorm disasters in coastal regions are related to the extreme sea level including storm surges, astronomical tides and waves (Fang et al. 2021; Hendry et al. 2019). Coastal rainstorm disaster risk may be underestimated if only the individual flood is considered (Wahl et al. 2015; Liu et al. 2022b). Therefore, further exploring how these different disaster chains influence and exacerbate each other would be valuable. In addition, the losses caused by different rainstorm disaster chains need to be analyzed. Through the comparison of risk assessment in Sect. 3.5, it can be seen that the construction of different disaster loss models leads to the uncertainty of risk assessment results.

In general, traditional statistical analysis methods for disaster chains have limitations. At present, there is a lack of research on the formation mechanism of rainstorm disaster chains by constructing mathematical and physical models. The quantitative analysis and the high-precision mathematical and physical models should be built to analyze rainstorm disaster chains (Liu et al. 2021b). With the cross-integration of multi-disciplines and multi-fields, as well as the improvement of data sharing ability across departments and industries, it is necessary to conduct more in-depth and detailed research on the rainstorm disaster chains in the GBA in the future. This study showed that the risk of rainstorm disasters in the GBA is high, and the accompanied losses are large. Therefore, the following mitigation strategies are proposed.

First, on the basis of disaster hazard, the exposure of disaster-bearing bodies and the sensitivity of disaster-pregnant environment should be fully considered, and the risk thresholds of rainstorm disasters and the critical values of rainstorm hazard in different cities need to be determined. Then, the early warning based on the risk of rainstorm disasters needs to be carried out.

Second, to deal with the increased risk of rainstorm disaster chain under climate change and urbanization, it is necessary to strengthen the construction of engineering measures to prevent rainstorm disasters, and different cities should have their own priorities. (1) The design standards of flood control and drainage systems should be improved. At present, most of the flood control standards in the GBA cities are less than once in 20 years (Chen et al. 2017). Under the situation of frequent extreme rainstorm events and frequent occurrence of excessive floods in the GBA (Qin et al. 2021), the flood prevention and waterlogging drainage capacity of urban river channels are obviously insufficient. (2) Dangerous reservoirs, dangerous dams of small- and medium-sized rivers, urban waterlogging points and the hidden danger points prone to landslides, debris flows and other disasters should be controlled in advance. (3) Geological disaster surveys in mountainous areas should be carried out to improve the monitoring, forecasting and early warning capabilities of rainstorms and related geological disasters.

Third, to deal with the risk of rainstorm disasters, non-engineering protection strategies have got increasing attention. Among the various rainstorm disaster chains in the GBA, rainstorm-induced urban waterlogging disaster chain is the most prominent. Accordingly, different cities should speed up the construction of sponge cities according to their actual conditions. Urban planning and layout should be scientific. We should rationally use urban natural water systems and increase green infrastructures such as urban green space and permeable surface. Urban rainstorm flood should be controlled through managing the

hydrological processes, such as infiltration, storage, purification, reuse and diversion, to alleviate the pressure of urban waterlogging (Wu et al. 2019; Chen et al. 2017).

5 Conclusions

In this study, we investigate the classification and mechanisms of rainstorm disaster chains, and analyze its spatiotemporal distribution characteristics based on the recorded rainstorm disasters during 1990–2018 in the GBA. Furthermore, we analyze the variations of rainstorm disaster risk factors such as hazard, disaster-pregnant environment and hazard-bearing bodies. Then, we establish quantitative function between DL and hazard index, and assess the risk level for different return periods. The main conclusions are as follows:

- 1) Rainstorms in the GBA can lead to disaster chains such as urban waterlogging, agricultural waterlogging, flash flood, riverine flood and debris flow/landslide. Among them, the urban waterlogging disaster chain has the highest probability, followed by the agricultural waterlogging, and the flash flood has the smallest probability. Since the twenty-first century, the frequency of urban waterlogging has increased and becomes the most prominent rainstorm disaster, while the frequency of flash flood, riverine flood and debris flow/landslide disaster chains has decreased. By jointly considering the rainstorm hazard, the exposure of disaster-bearing bodies and the sensitivity of disaster-pregnant environment, Shenzhen, Zhaoqing and Huizhou rank the top three in the frequency of rainstorm disaster chains.
- 2) The rainstorm disaster chains are influenced and exacerbated by each other, leading to cascading effects in different disaster-bearing bodies. During 1990–2018, the frequency of 2, 3 and 4 disaster chains accounts for 30%, 7.9% and 0.4% of the total rainstorm-induced disasters in the GBA, respectively. The city with the most frequent compound disaster chains is Zhaoqing, accounting for 54.1% of its total rainstorm disaster chains. The concurrence of four disaster chains only appears in Guangzhou and Jiangmen in recent 30 years.
- 3) From 1990 to 2018, the rainstorm disaster loss index in the GBA has shown a significantly increasing trend ($p < 0.05$), and the inter-annual fluctuation is large. As for the multi-year averaged rainstorm disaster loss index, it is the highest in Zhaoqing and the lowest in Zhuhai. The assessment of rainstorm disaster risk shows that the areas at high-risk level increase with the augmentation of return period in the GBA. In general, Guangzhou, Zhaoqing and Shenzhen are at high-risk level for 10-year and 20-year return periods.

Acknowledgements This work was supported by the National Key R&D Program of China (Grant No. 2019YFC1510400). We thank professor Clague, Editor-in-Chief, and four anonymous reviewers who all made very valuable suggestions for improvement of this manuscript. We thank Nanjing Hurricane Translation for reviewing the English language quality of this paper.

Author contributions All authors contributed to the study conception and design. Material preparation, data collection and analysis were performed by YW, GG, JZ, QL and LS. The first draft of the manuscript was written by YW, and all authors commented on previous versions of the manuscript. All authors read and approved the final manuscript.

Funding This work was supported by the National Key R&D Program of China (2019YFC1510400).

Data availability The data that support the findings of this study are openly available on websites (www.resdc.cn and www.data.cma.cn).

Declarations

Conflict of interest The authors have no conflicts of interest to declare that are relevant to the content of this article.

References

- Canters F, Vanderhaegen S, Khan AZ, Engelen G, Uljee L (2014) Land-use simulation as a supporting tool for flood risk assessment and coastal safety planning: the case of the Belgian coast. *Ocean Coast Manag* 101:102–113
- Cardona OD, Aalst MK, Birkmann J, Fordham M, McGregor G, Perez R, Pulwarty RS (2012) Determinants of risk: exposure and vulnerability. Cambridge University Press, Cambridge
- Chen YB, Qin J, Dong L, Zhang T (2017) The formation regularity and control measures of urban pluvial floods in Guangzhou City. *China Flood Drought Manag* 27(5):72–76
- Chen YM, Xie W, Xu XC (2019) Changes of population, built-up land, and cropland exposure to natural hazards in China from 1995 to 2015. *Int J Disaster Risk Sci* 10:557–572
- China Meteorological Administration (2020) China meteorological disaster yearbook 2019. China Meteorological Press, Beijing
- Du ZQ, Gu JY (2016) A domain ontology construction method of disaster chain: case study of rainstorm flood disaster chain. *Geomat World* 23(4):7–13
- Fang J, Meng MJ, Wang JG, Shi PJ (2015) Assessment and mapping of global fluvial flood risk. *J Nat Disasters* 24(1):1–8
- Fang J, Wahl T, Fang J, Sun X, Kong F, Liu M (2021) Compound flood potential from storm surge and heavy precipitation in coastal China: dependence, drivers, and impacts. *Hydrol Earth Syst Sci* 25:4403–4416
- Feng SS, Fan FL (2018) Spatial-temporal changes of impervious surface in the Guangdong–Hong Kong–Macao Greater Bay Area during 2006–2016. *Tropical Geogr* 38(4):536–545
- Golnaraghi M, Etienne C, Sapir DG (2014) Atlas of mortality and economic losses from weather, climate and water extremes (1970–2012). World Meteorological Organization. http://www.wmo.int/pages/prog/drr/transfer/2014.06.12-WMO1123_Atlas_120614.pdf
- Guangdong Provincial Department of Land and Resources (2018) Geological disaster prevention plan of Guangdong Province in 2018
- Hallegatte S (2014) Modeling the roles of heterogeneity, substitution, and inventories in the assessment of natural disaster economic costs. *Risk Anal* 34:152–167
- Helbing D (2013) Globally networked risks and how to respond. *Nature* 497:51–59
- Hendry A, Haigh ID, Nicholls RJ, Winter H, Neal R, Wahl T, Joly-Laugel A, Darby SE (2019) Assessing the characteristics and drivers of compound flooding events around the UK coast. *Hydrol Earth Syst Sci* 23:3117–3139
- Islam MR, Raja DR (2021) Waterlogging risk assessment: an undervalued disaster risk in coastal urban community of Chattogram, Bangladesh. *Earth* 2:151–173
- Kang Y, Park CS, Park JY, Cho D (2018) Spatial differences in the heavy precipitation risk intensity in South Korea. *Hum Ecol Risk Assess* 24:1579–1594
- Kappes MS, Keiler M, Elverfeldt V, Glade T, Murty TS (2012) Challenges of analyzing multi-hazard risk: a review. *Nat Hazards* 64(2):1925–1958
- Levermann A (2014) Make supply chains climate-smart. *Nature* 506:27–29
- Li Y, Zhao SS (2022) Floods losses and hazards in China from 2001 to 2020. *Clim Change Res* 18(2):154–165
- Li ZH, Song KY, Peng L (2021) Flood risk assessment under land use and climate change in Wuhan City of the Yangtze River Basin. *China Land* 10:878
- Liu BJ, Chen JF, Lu WX, Chen XH, Lian YQ (2016) Spatiotemporal characteristics of precipitation changes in the Pearl River Basin, China. *Theor Appl Climatol* 123:537–550

- Liu F, Liu X, Xu T, Yang G, Zhao YL (2021a) Driving factors and risk assessment of rainstorm waterlogging in urban agglomeration areas: a case study of the Guangdong–Hong Kong–Macao Greater Bay Area. *China Water* 13(6):770
- Liu YZ, Tang WW, Zhang WT, Zhang XN, Niu S (2021b) Review of flood disaster risk analysis based on disaster chain. *Water Resour Prot* 37(1):20–27
- Liu Q, Xu H, Wang J (2022a) Assessing tropical cyclone compound flood risk using hydrodynamic modelling: a case study in Haikou City. *China Nat Hazards Earth Syst Sci* 22:665–675
- Liu T, Shi P, Fang J (2022b) Spatiotemporal variation in global floods with different affected areas and the contribution of influencing factors to flood-induced mortality (1985–2019). *Nat Hazards* 111:2601–2625
- Lyu HM, Sun WJ, Shen SL, Arulrajah A (2018) Flood risk assessment in metro systems of mega-cities using a GIS-based modeling approach. *Sci Total Environ* 626:1012–1025
- Metin AD, Dung NV, Schröter K, Guse B, Apel H, Kreibich H, Vorogushyn S, Merz B (2018) How do changes along the risk chain affect flood risk? *Nat Hazards Earth Syst Sci* 18:3089–3108
- Qin DH, Zhang JY, Shan CC, Song LC (2015) China national assessment report on risk management and adaptation of climate extremes and disasters. Science Press, Beijing
- Qin DH, Ding YJ, Zhai PM (2021) Climate and ecological environment evolution in China: 2021. The second volume, Science Press, Beijing
- Quan RS (2014) Rainstorm waterlogging risk assessment in central Urban area of Shanghai based on multiple scenario simulation. *Nat Hazards* 73:1569–1585
- Ren Z, Yu Y, Zou F, Xu Y (2012) Quality detection of surface historical basic meteorological data. *J Appl Meteor Sci* 23(6):739–747
- Samphantharak K (2014) Natural disasters and the economy: some recent experiences from Southeast Asia. *Asian Pac Econ Lit* 28(2):33–51
- Shi PJ (2005) Theory and practice on disaster system research in a fourth time. *J Nat Disasters* 14(6):1–7
- Shi XJ, Zha XC, Liu JH, Wang G (2017) Cloud model-based risk assessment of flood disasters in Ankang City on upper reaches of Hanjiang River. *Adv Sci Technol Water Resour* 37(3):29–34
- Silva SF, Martinho M, Capitão R, Reis T, Fortes CJ, Ferreira GC (2017) An index based method for coastal-flood risk assessment in low-lying areas. *Ocean Coast Manag* 144:90–104
- Sun A, Zhai JQ, Li Y, Huang DP, Wang GF (2020) Urban waterlogging risk assessment in well-developed region of Eastern China. *Phys Chem Earth* 115:102824
- Tang Y (2016) Analysis of hidden dangers from geological hazards, and safety recommendations in Shenzhen. *Shanghai Land Res* 37(3):82–85
- Wahl T, Jain S, Bender J, Meyers SD, Luther ME (2015) Increasing risk of compound flooding from storm surge and rainfall for major US cities. *Nat Clim Change* 5:1093–1097
- Wan HL, Song HL, Zhu CC (2018) Spatio-temporal evolution of drought and flood disaster chains in Baoji area from 1368 to 1911. *J Geog Sci* 28(3):337–350
- Wang DH, Liu JJ, Shan YL, Ji JP, Song HY (2001) The design and establishment of 1:250000 digital elevation model of China. *Bull Surv Mapp* 10:27–29
- Wang M, Tian WP, Cui YQ (2011) Case analysis of rainstorm disaster chain in Shaanxi Province and comprehensive disaster reduction measures. *Transp Enterprise Manag* 26(7):69–71
- Wang H, Liu GF, Wang HM (2014) Risk assessment of urban extreme rain and flood disaster based on cloud model. *J Econ Water Resour* 2:15–18
- Wang YJ, Han ZY, Gao R (2021) Changes of extreme high temperature and heavy precipitation in the Guangdong–Hong Kong–Macao Greater Bay Area. *Geomat Nat Haz Risk* 12(1):1101–1126
- Wang YJ, Zhai JQ, Gao G, Liu GF, Song LC (2022) Risk assessment of rainstorm disasters in the Guangdong–Hong Kong–Macao Greater Bay Area of China during 1990–2018. *Geomat Nat Haz Risk* 13(1):267–288
- Wen QP, Zhou YH, Huo ZG, Li L, Fang SD, Shi RQ, Che Q (2018) Quantitative assessment on vulnerability of storm flood disasters in Hubei Province. *Chin J Agrometeorol* 39(8):547–557
- Willner SN, Otto C, Levermann A (2018) Global economic response to river floods. *Nat Clim Change* 8:594–598
- Wu HY, Zou Y, Liu W (2019) Quantitative assessment of regional heavy rainfall process in Guangdong and its climatological characteristics. *J Appl Meteorol Sci* 30(2):233–244
- Xu XL, Liu JY, Zhang SW, Li RD, Yan CZ, Wu SX (2018) China multi-period land use land cover remote sensing monitoring data set (CNLUCC). The data registration and publishing system of the resource and environmental science data center of the Chinese academy of sciences (<http://www.resdc.cn>). <https://doi.org/10.12078/2018070201.2018>
- Yang C, Li Q, Zhao T, Liu H, Gao W, Shi T, Guan M, Wu G (2017) Detecting spatiotemporal features and rationalities of urban expansions within the Guangdong–Hong Kong–Macao Greater Bay Area

- of China from 1987 to 2017 using time-series Landsat images and socioeconomic data. *Remote Sens* 11:2215
- Ye LM, Zhou YH, Zhou Y (2018) Instance analysis of rainstorm floods chain and chain-cutting disaster mitigation building. *J Catastr* 33(1):65–70
- Ye DX, Wang ZY, Gao R, Wang R, Xiao C (2019) Objective identification and climatic characters of the regional rainstorm event in China from 1961 to 2016. *Clim Change Res* 15(6):575–583
- Yu Y, Li F (2010) A study on the effect of agro-meteorological disasters on China's grain yield based on panel data. *Econ Manag* 24(11):5–8
- Zhang Q, Singh VP, Peng JT, Chen YQ, Li JF (2012) Spatial-temporal changes of precipitation structure across the Pearl River basin, China. *J Hydrol* 440–441:113–122
- Zhao Y, Zou X, Cao L, Xu X (2014) Changes in precipitation extremes over the Pearl River Basin, southern China, during 1960–2012. *Quatern Int* 333:26–39
- Zhao YJ, Zhen FL, Yao YQ, Zhang JQ (2022) Spatio-temporal change characteristics of agrometeorology disasters in whole country from 1978 to 2018. *J Nat Disasters* 31(1):198–207
- Zhou L, Wu XH, Ji ZH, Gao G (2017) Characteristic analysis of rainstorm-induced catastrophe and the countermeasures of flood hazard mitigation about Shenzhen city. *Geomat Nat Haz Risk* 8(2):1886–1897
- Zhou B, Zeng H, Zhao L, Han Z (2019) Climate change and climate risks in the Guangdong–Hong Kong–Macao Greater Bay Area. Annual report on actions to address climate change. pp 239–258

Publisher's Note Springer Nature remains neutral with regard to jurisdictional claims in published maps and institutional affiliations.

Springer Nature or its licensor (e.g. a society or other partner) holds exclusive rights to this article under a publishing agreement with the author(s) or other rightsholder(s); author self-archiving of the accepted manuscript version of this article is solely governed by the terms of such publishing agreement and applicable law.

Authors and Affiliations

Yujie Wang^{1,2} · Ge Gao^{1,3} · Jianqing Zhai³ · Qiufeng Liu³ · Lianchun Song³

✉ Ge Gao
gaoge@cma.gov.cn

¹ Key Laboratory of Meteorological Disaster, Ministry of Education/International Joint Research Laboratory on Climate and Environment Change/Collaborative Innovation Center on Forecast and Evaluation of Meteorological Disasters (CIC-FEMD), Nanjing University of Information Science & Technology, Nanjing 210044, China

² School of Atmospheric Sciences, Nanjing University of Information Science and Technology, Nanjing 210044, China

³ National Climate Center, China Meteorological Administration, Beijing 100081, China